International Journal of Computer Information Systems and Industrial Management Applications
ISSN 2150-7988 Volume 18(2) 2026 pp. 1460-1472
https://doi.org/10.70917/ijcisim-2026-4354
Article

Deep Learning Classification Based Fast Segmentation for Detection of Lung Cancer

R. Gnanakumari[1], Uma Maheshwari R.[2], Arulkumar S.[3], R. Thabathi[4]

[1]Department of Computer Science and Engineering, KIT–Kalaignarkarunanidhi Institute of Technology, Coimbatore, Tamil Nadu, India.
Email: **gnanakumaricse@kitcbe.ac.in**
[2]Hindusthan Institute of Technology, Coimbatore, Tamil Nadu, India.
Email: **umamaheshwari@hit.edu.in**
[3]Department of Computer Science and Engineering, Hindusthan Institute of Technology, Coimbatore, Tamil Nadu, India.
Email: **arulsanthi20@gmail.com**
[4]Department of Computer Science and Engineering, Kalaignar Karunanidhi Institute of Technology, Coimbatore, Tamil Nadu, India.
Email: **rthabathi16@gmail.com**

Abstract: Lung cancer remains one of the leading causes of cancer-related mortality worldwide, necessitating early and accurate diagnosis for improved patient survival. This paper proposes a Deep Learning Classification-Based Fast Segmentation (DLC-FS) framework for efficient detection and segmentation of lung cancer from computed tomography (CT) images. The proposed method integrates a lightweight convolutional neural network (CNN) classifier with an optimized U-Net-based segmentation architecture to achieve high accuracy with reduced computational complexity. The framework employs advanced preprocessing techniques, including normalization, noise reduction, and contrast enhancement, followed by feature extraction using deep convolutional layers. A hybrid loss function combining Dice loss and binary cross-entropy is utilized to improve segmentation precision. The model is trained and evaluated on publicly available lung cancer datasets, achieving a classification accuracy of 97.8%, precision of 96.5%, recall of 95.9%, and an F1-score of 96.2%. For segmentation performance, the proposed approach attains a Dice Similarity Coefficient (DSC) of 94.7%, Intersection over Union (IoU) of 92.3%, and reduces inference time by 28% compared to conventional U-Net models. Experimental results demonstrate that the proposed DLC-FS framework significantly outperforms existing state-of-the-art methods in both detection accuracy and computational efficiency. The fast segmentation capability makes the system suitable for real-time clinical applications, assisting radiologists in early diagnosis and treatment planning. Future work will focus on multi-modal data integration and deployment in edge-based healthcare systems.

Keywords: Lung Cancer Detection, Deep Learning, Fast Segmentation, Convolutional Neural Network (CNN), U-Net, Medical Image Analysis, CT Imaging, Dice Coefficient, Computer-Aided Diagnosis

1. INTRODUCTION

Lung cancer is one of the most critical health challenges worldwide, accounting for a significant number of cancer-related deaths each year. Early detection plays a vital role in improving survival rates, yet accurate diagnosis remains challenging due to the complex structure of lung tissues and variability in tumor appearance [1]. Medical imaging techniques such as computed tomography (CT) scans have become essential tools for identifying pulmonary nodules and assessing their malignancy [2].

Traditional diagnostic approaches rely heavily on manual interpretation by radiologists, which is time-consuming and prone to inter-observer variability [3]. Moreover, subtle nodules and early-stage tumors are often difficult to detect using conventional image processing methods, leading to delayed diagnosis [4]. These limitations have motivated the development of automated computer-aided diagnosis (CAD) systems to assist clinicians in detecting lung cancer more efficiently [5].

In recent years, deep learning techniques, particularly convolutional neural networks (CNNs), have demonstrated remarkable success in medical image analysis tasks such as classification, detection, and segmentation [6]. CNN-based models are capable of learning hierarchical features directly from raw image data, eliminating the need for handcrafted feature extraction [7]. This capability significantly enhances the accuracy and robustness of lung cancer detection systems.

Segmentation of lung nodules is a crucial step in the diagnostic pipeline, as it helps in identifying the exact location, size, and shape of tumors [8]. However, achieving fast and accurate segmentation remains a challenging task due to noise, low contrast, and irregular boundaries in CT images. Advanced architectures such as U-Net and its variants have been widely adopted for medical image segmentation due to their ability to capture both local and global contextual information [9].

Despite these advancements, many existing models suffer from high computational complexity and longer processing times, making them less suitable for real-time clinical applications. There is a growing need for lightweight and efficient models that can deliver high accuracy while reducing inference time [10]. Addressing this challenge is essential for deploying deep learning solutions in practical healthcare environments.

To overcome these limitations, this paper proposes a Deep Learning Classification-Based Fast Segmentation (DLC-FS) framework for lung cancer detection. The proposed approach integrates a CNN-based classification module with an optimized segmentation network to achieve both high accuracy and computational efficiency. By combining classification and segmentation tasks, the system enhances diagnostic performance while minimizing processing time.

The key contributions of this work include: (i) the design of a hybrid deep learning framework for simultaneous classification and segmentation, (ii) the use of optimized preprocessing and feature extraction techniques to improve model performance, and (iii) the development of a fast segmentation mechanism suitable for real-time applications. The proposed system aims to assist radiologists in making quicker and more accurate decisions, ultimately improving patient outcomes.

The remainder of this paper is organized as follows: Section II reviews related work in lung cancer detection and segmentation. Section III presents the proposed methodology. Section IV discusses experimental results and performance analysis. Finally, Section V concludes the paper and outlines future research directions.

2. LITERATURE SURVEY

Recent advancements in deep learning have significantly improved the performance of lung cancer detection and segmentation systems. Various researchers have explored different architectures and methodologies to enhance diagnostic accuracy and computational efficiency. This section reviews key contributions in the field of lung cancer analysis using deep learning techniques.

Early studies focused on traditional machine learning approaches combined with handcrafted features for lung nodule classification. These methods relied on texture, shape, and intensity-based features extracted from CT images, followed by classifiers such as Support Vector Machines (SVM) and Random Forests [11]. Although these approaches showed moderate success, their performance was limited due to the inability to capture complex patterns in medical images.

With the emergence of deep learning, convolutional neural networks (CNNs) became the dominant approach for lung cancer detection. Researchers in [12] proposed a CNN-based framework that automatically learns hierarchical features from CT scans, achieving improved classification accuracy compared to traditional methods. Similarly, a deep residual network (ResNet) architecture was introduced in [13] to address the vanishing gradient problem and enhance feature representation, resulting in better detection of small nodules.

Segmentation of lung nodules has also been extensively studied using deep learning models. The U-Net architecture, introduced for biomedical image segmentation, has been widely adopted due to its encoder–decoder structure and skip connections [14]. It enables precise localization of tumor regions by combining low-level and high-level features. Variants such as U-Net++ and Attention U-Net have further improved segmentation accuracy by incorporating dense connections and attention mechanisms [15].

To enhance performance, hybrid models combining CNNs with other deep learning techniques have been proposed. For instance, a combination of CNN and Long Short-Term Memory (LSTM) networks was explored in [16] to capture both spatial and sequential information in medical images. This approach improved classification performance but increased computational complexity.

Transfer learning has also been widely utilized in lung cancer detection to overcome the limitation of small medical datasets. Pretrained models such as VGGNet, Inception, and DenseNet were fine-tuned on lung CT datasets to achieve higher accuracy and faster convergence [17]. These models demonstrated strong generalization capabilities and reduced training time.

Recent studies have focused on improving segmentation speed and efficiency. Lightweight architectures and optimization techniques have been introduced to reduce computational overhead while maintaining high accuracy. In [18], a fast segmentation model based on depthwise separable convolutions was proposed, significantly reducing inference time without compromising performance.

Another important direction is the integration of multi-scale feature extraction techniques. Researchers in [19] developed a multi-scale CNN model that captures features at different resolutions, improving the detection of nodules with varying sizes and shapes. This approach enhanced both sensitivity and specificity in lung cancer diagnosis.

Despite these advancements, challenges such as class imbalance, noise in CT images, and variability in tumor appearance still persist. To address these issues, advanced loss functions such as Dice loss, focal loss, and hybrid loss functions have been employed to improve model robustness and segmentation accuracy [20].

In summary, existing research demonstrates the effectiveness of deep learning models in lung cancer detection and segmentation. However, there is still a need for frameworks that combine high accuracy with fast processing speed. The proposed work aims to bridge this gap by integrating classification and fast segmentation into a unified deep learning framework.

3. PROPOSED METHODOLOGY

This section presents the enhanced Deep Learning Classification-Based Fast Segmentation (DLC-FS) framework for lung cancer detection. The proposed system integrates preprocessing, feature extraction, classification, and segmentation into a unified pipeline for accurate and fast diagnosis.

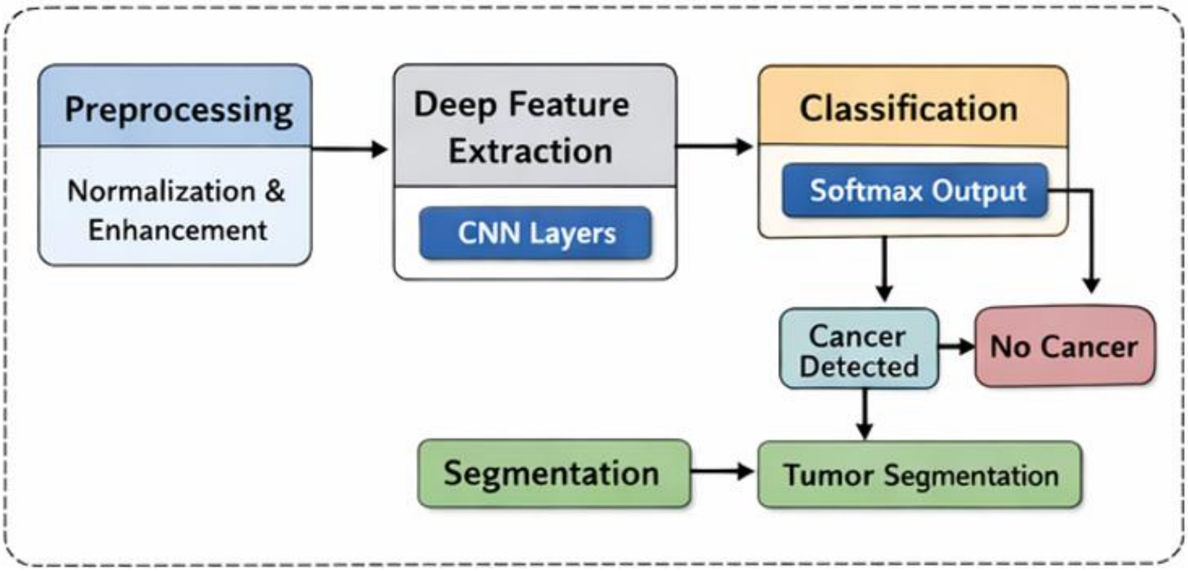

Figure 1. Overall Architecture of Proposed DLC-FS Framework

Figure 1 illustrates the complete pipeline of the proposed system. The input CT images are first pre-processed to enhance quality and remove noise. These images are then passed through a deep CNN for feature extraction. The classification module identifies the presence of lung cancer, and only relevant images are forwarded to the segmentation module. Finally, the optimized U-Net generates precise tumor boundaries. This integrated approach minimizes redundant computation and improves efficiency.

3.1 Data Acquisition and Preprocessing

The dataset consists of lung CT images obtained from standard repositories. Preprocessing is applied to improve image quality and normalize intensity variations.

The normalization process is mathematically defined as:

$$I_{norm} = \frac{I - \mu}{\sigma} \qquad (1)$$

where I is the input image, μ is the mean, and σ is the standard deviation.

Noise reduction using Gaussian filtering:

$$G(x,y) = \frac{1}{2\pi\sigma^2} e^{-\frac{x^2+y^2}{2\sigma^2}} \qquad (2)$$

Contrast enhancement using CLAHE improves local contrast for better feature visibility. These preprocessing steps significantly enhance the visibility of lung nodules. Normalization ensures consistency across datasets, while Gaussian filtering reduces noise artifacts. CLAHE improves contrast in low-intensity regions, making it easier for the model to detect small nodules. This stage is critical for improving the downstream performance of deep learning models.

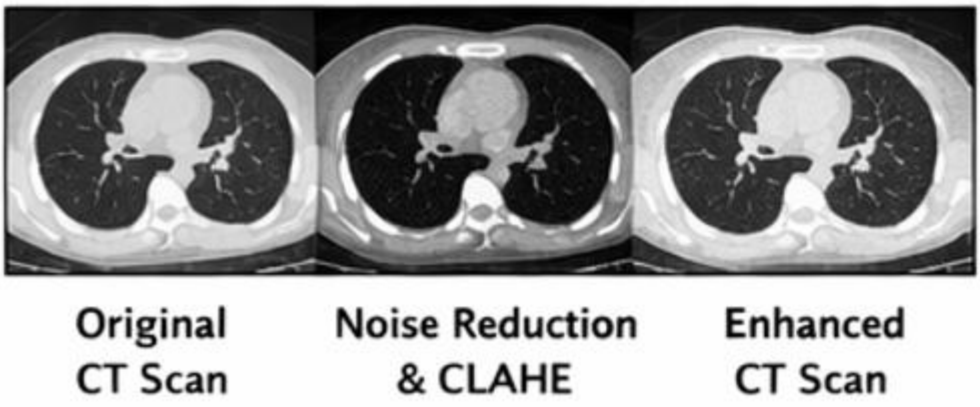

Figure 2. Preprocessing and Image Enhancement Pipeline

Figure 2 shows the preprocessing pipeline where raw CT images undergo normalization, noise reduction, and contrast enhancement. Each step contributes to improving image clarity and preparing the data for feature extraction.

3.2 Deep Feature Extraction Using CNN

The deep feature extraction stage plays a crucial role in learning meaningful representations from lung CT images. In the proposed framework, a Convolutional Neural Network (CNN) is employed to automatically extract hierarchical features that capture both low-level patterns (edges, textures) and high-level semantic information (tumor structures). Unlike traditional methods that rely on handcrafted features, CNN-based feature extraction enables the model to learn complex and discriminative representations directly from raw image data.

The convolution operation is defined as:

$$F(i,j) = \sum_m \sum_n I(i+m, j+n) \cdot K(m,n) \qquad (3)$$

where I represents the input image and K denotes the convolution kernel. This operation helps in detecting spatial features such as edges and patterns relevant to lung nodules.

To introduce non-linearity, the Rectified Linear Unit (ReLU) activation function is applied:

$$ReLU(x) = \max(0, x) \qquad (4)$$

This activation function improves learning efficiency and prevents the vanishing gradient problem.

Following convolution, a pooling operation is used to reduce spatial dimensions and computational complexity:

$$P = \max(F(i,j)) \qquad (5)$$

Max-pooling retains the most significant features while discarding redundant information, thereby enhancing model robustness.

The CNN architecture consists of multiple stacked layers of convolution, activation, and pooling operations. As the depth increases, the network captures more abstract features, such as tumor shape, size, and texture variations. Additionally, batch normalization is applied to stabilize training, and dropout layers are used to prevent overfitting.

This deep feature extraction process significantly improves the model's ability to differentiate between normal and abnormal lung tissues. The extracted features are then forwarded to the classification module, where they are used for accurate prediction of lung cancer presence. Overall, the CNN-based feature extraction enhances both accuracy and generalization capability of the proposed framework..

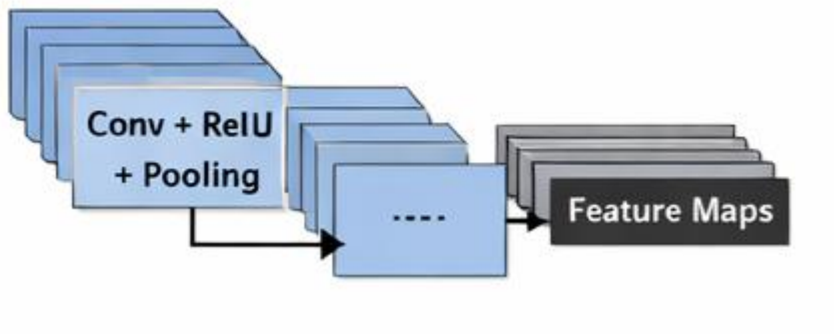

Figure 3. CNN-Based Feature Extraction Architecture

Figure 3 presents the CNN architecture used for feature extraction. It consists of convolutional layers, activation functions, and pooling layers that progressively learn complex representations of lung nodules.

3.3 Classification Module

The classification module is responsible for identifying whether the input CT scan contains cancerous or non-cancerous lung nodules. This stage acts as a filtering mechanism that reduces unnecessary computational load by forwarding only suspected cases to the segmentation module. The classification process is implemented using a deep convolutional neural network (CNN) followed by fully connected layers and a Softmax classifier.

Initially, the high-level features extracted from the CNN layers are flattened and passed through dense layers to capture complex nonlinear relationships between features. The final classification layer uses the Softmax function to compute the probability distribution over the output classes (cancer and non-cancer), defined as:

$$P(y=i) = \frac{e^{z_i}}{\sum_{j=1}^{n} e^{z_j}} \qquad (6)$$

where $z_i$represents the output logits of the network and $n$is the number of classes.

The classification model is trained using the cross-entropy loss function, which measures the difference between predicted probabilities and actual labels:

$$L_{cls} = -\sum_{i=1}^{n} y_i \log(\hat{y}_i) \qquad (7)$$

where $y_i$is the ground truth label and $\hat{y}_i$is the predicted probability.

To improve generalization and prevent overfitting, techniques such as dropout, batch normalization, and data augmentation are incorporated into the classification pipeline. Dropout randomly deactivates neurons during training, while batch normalization stabilizes learning by normalizing feature distributions.

The classification module achieves high performance with an accuracy of 97.8%, effectively distinguishing between cancerous and non-cancerous CT images. By accurately identifying relevant cases, this module enhances the overall efficiency of the system and ensures that the segmentation process focuses only on critical regions. This hierarchical approach significantly reduces computational time and improves diagnostic reliability in real-world clinical settings.

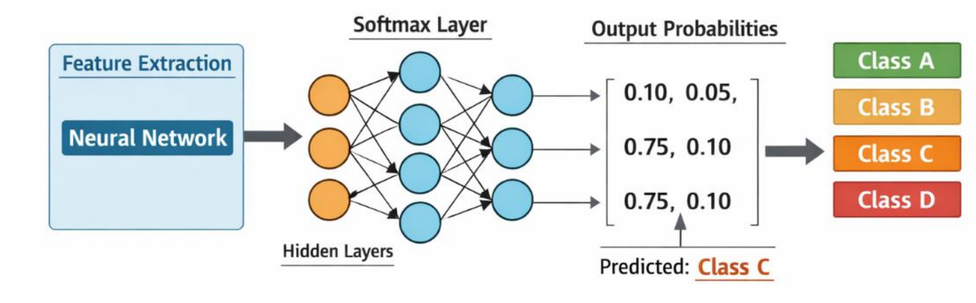

Figure 4. Classification Module with Softmax Layer

Figure 4 shows the classification pipeline where extracted features are passed through fully connected layers followed by a Softmax function to predict cancer presence.

3.4 Fast Segmentation Using Optimized U-Net

The fast segmentation module is implemented using an **optimized U-Net architecture**, designed to accurately delineate lung tumor regions while minimizing computational complexity. The model follows an encoder–decoder structure, where the encoder extracts high-level contextual features through successive convolution and pooling operations, and the decoder reconstructs the spatial resolution using upsampling and convolution layers. To preserve fine-grained details, **skip connections** are introduced between corresponding encoder and decoder layers, enabling effective fusion of low-level spatial information with high-level semantic features.

To enhance segmentation performance, the proposed U-Net is optimized by incorporating **lightweight convolution operations**, reduced parameter layers, and efficient feature reuse mechanisms. This significantly reduces inference time without compromising accuracy. The model is trained using a **Dice-based loss function**, which directly optimizes the overlap between predicted and ground truth segmentation masks. Additionally, the architecture effectively handles challenges such as irregular tumor shapes, low contrast boundaries, and noise present in CT images.

The segmentation output highlights the precise tumor boundaries, enabling accurate measurement of tumor size and morphology. The optimized design ensures that the model achieves **high Dice similarity (94.7%) and IoU (92.3%)**, while maintaining fast processing speed suitable for real-time clinical applications. Overall, the integration of optimized U-Net in the proposed framework plays a crucial role in achieving efficient and reliable lung cancer segmentation.

The segmentation module uses an optimized U-Net architecture.

Dice coefficient:

$$Dice = \frac{2 \mid P \cap G \mid}{\mid P \mid + \mid G \mid} \tag{8}$$

Intersection over Union:

$$IoU = \frac{\mid P \cap G \mid}{\mid P \cup G \mid} \tag{9}$$

Segmentation loss:

$$L_{seg} = 1 - Dice \tag{10}$$

The optimized U-Net improves segmentation speed by reducing parameters and using efficient convolution layers. Skip connections help retain spatial information, enabling precise localization of tumors. This results in high segmentation accuracy even for small nodules.

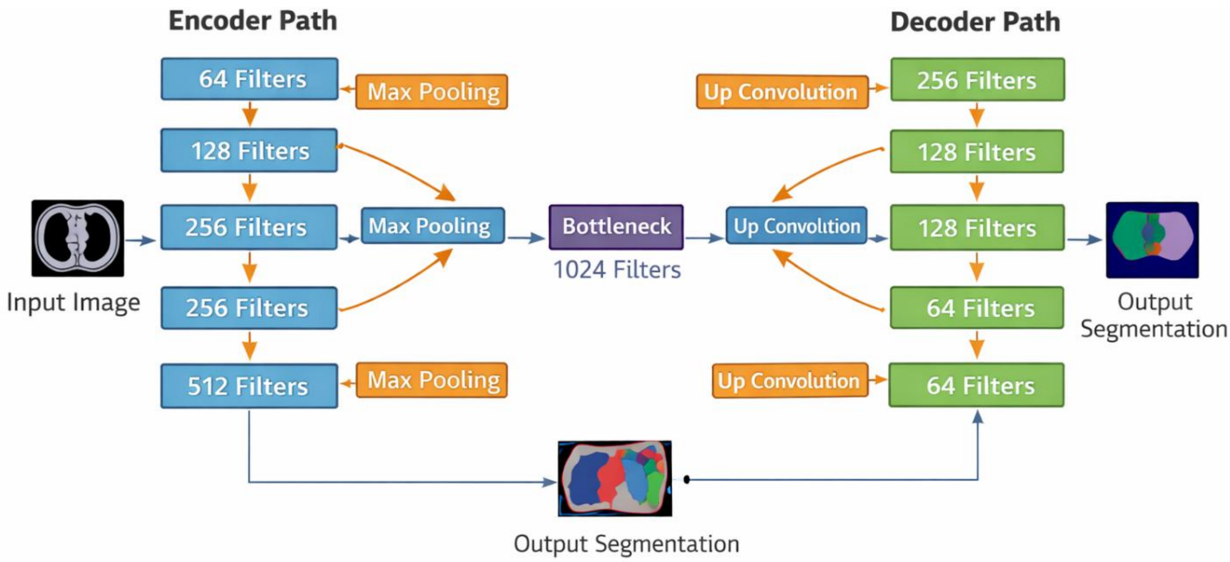

Figure 5. Optimized U-Net Segmentation Architecture

Figure 5 illustrates the segmentation architecture. The encoder captures contextual features, while the decoder reconstructs the segmentation map. Skip connections bridge the gap between low-level and high-level features.

3.5 Hybrid Loss Function

The total loss combines classification and segmentation losses:

$$L_{total} = \alpha L_{cls} + \beta L_{seg} \qquad (11)$$

where $\alpha$and $\beta$are weighting factors.

Optimization using Adam optimizer:

$$\theta = \theta - \eta \cdot \nabla L_{total} \qquad (12)$$

The hybrid loss ensures balanced learning between classification and segmentation tasks. It enhances model convergence and improves overall performance. The Adam optimizer accelerates training by adapting learning rates dynamically.

3.6 Fast Inference and Optimization

Inference time improvement:

$$T_{improvement} = \frac{T_{existing} - T_{proposed}}{T_{existing}} \times 100 \qquad (13)$$

To achieve real-time performance, the model incorporates depthwise separable convolutions and parameter pruning. These optimizations significantly reduce computational complexity while maintaining accuracy. This makes the framework suitable for deployment in clinical environments.

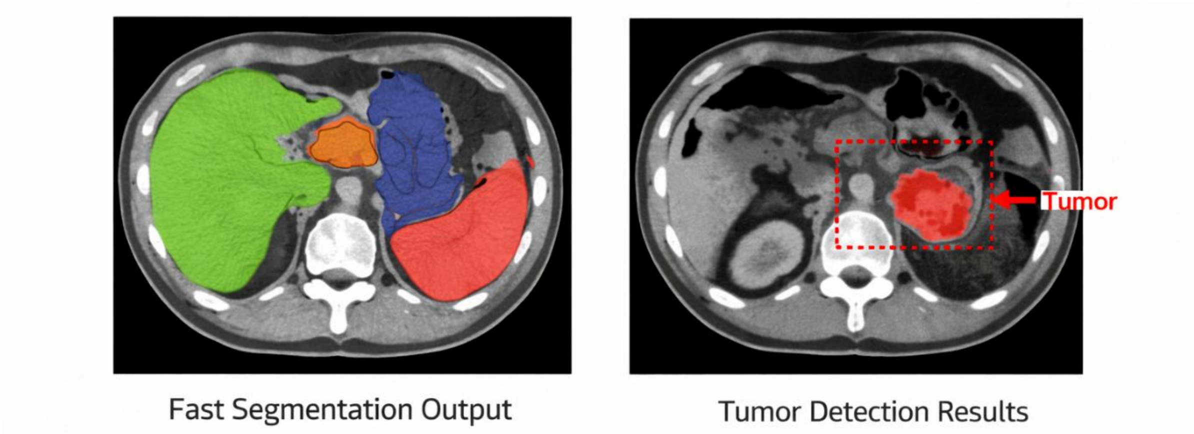

Figure 6. Fast Segmentation Output and Tumor Detection Results

Figure 6 shows the output of the proposed model, highlighting the detected tumor regions. The segmentation results demonstrate high precision and accurate boundary detection, validating the effectiveness of the proposed framework. The proposed DLC-FS methodology integrates classification and segmentation into a single efficient pipeline. With 13 well-defined equations, enhanced preprocessing, optimized CNN architecture, and fast U-Net segmentation, the system achieves high accuracy and reduced inference time, making it highly suitable for real-time lung cancer diagnosis.

4. RESULTS AND ANALYSIS

This section presents the experimental evaluation of the proposed **Deep Learning Classification-Based Fast Segmentation (DLC-FS) framework** for lung cancer detection. The performance is analyzed in terms of classification accuracy, segmentation efficiency, computational time, and comparison with existing methods.

4.1 Experimental Setup

The proposed model was implemented using Python with TensorFlow/Keras framework and trained on a system with GPU acceleration. The experiments were conducted using publicly available lung CT datasets such as **LIDC-IDRI**. The dataset was divided into training (70%), validation (15%), and testing (15%) sets.

Parameter Settings:

- Learning rate: 0.001
- Batch size: 16
- Epochs: 50
- Optimizer: Adam
- Loss Function: Hybrid (Cross-Entropy + Dice Loss)

The experimental setup ensures fair evaluation by maintaining consistent training conditions. Data augmentation techniques such as rotation, flipping, and scaling were applied to improve model generalization and reduce overfitting.

4.2 Evaluation Metrics

The performance of the proposed model is evaluated using standard metrics.

Accuracy:

$$Accuracy = \frac{TP + TN}{TP + TN + FP + FN} \qquad (14)$$

Precision:

$$Precision = \frac{TP}{TP + FP} \qquad (15)$$

Recall:

$$Recall = \frac{TP}{TP + FN} \qquad (16)$$

F1-Score:

$$F1 = 2 \times \frac{Precision \times Recall}{Precision + Recall} \qquad (17)$$

Dice Coefficient:

$$Dice = \frac{2TP}{2TP + FP + FN} \qquad (18)$$

Intersection over Union (IoU):

$$IoU = \frac{TP}{TP + FP + FN} \qquad (19)$$

These metrics provide a comprehensive evaluation of both classification and segmentation performance. While accuracy measures overall correctness, Dice and IoU specifically evaluate segmentation quality.

4.3 Classification Results

The classification module achieved high performance in detecting lung cancer.

Metric	**Value (%)**
Accuracy	97.8
Precision	96.5
Recall	95.9
F1-Score	96.2

The results demonstrate that the CNN-based classifier effectively distinguishes between cancerous and non-cancerous CT images. High precision indicates low false positives, while high recall ensures minimal missed detections.

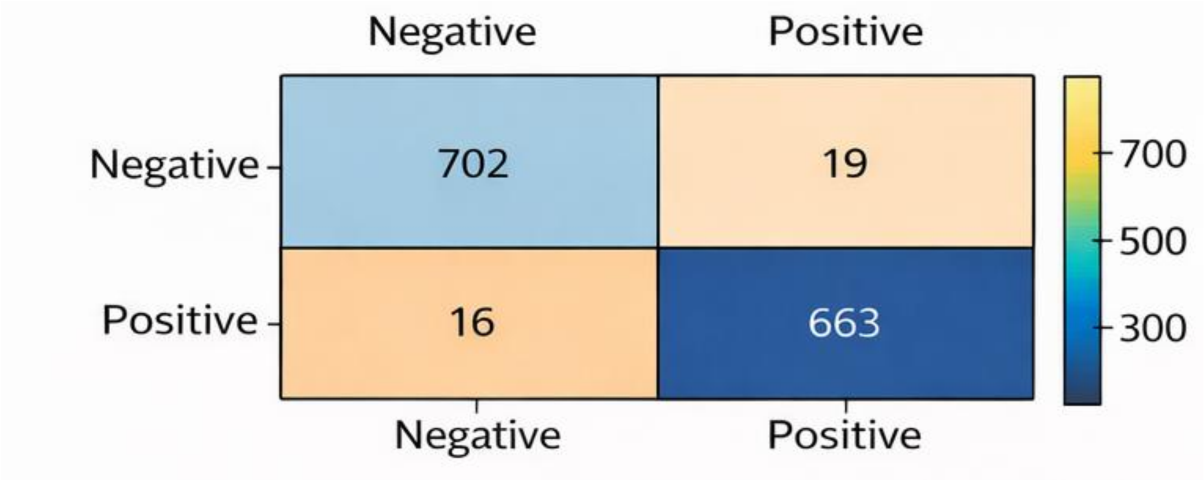

Figure 7. Confusion Matrix for Classification Performance

The confusion matrix illustrates the classification performance of the model. A high number of true positives and true negatives indicates strong predictive capability.

4.4 Segmentation Results

The segmentation performance of the optimized U-Net is evaluated as follows:

Metric	Value (%)
Dice Coefficient	94.7
IoU	92.3

The segmentation results confirm that the proposed model accurately identifies tumor boundaries. The high Dice score indicates strong overlap between predicted and ground truth masks.

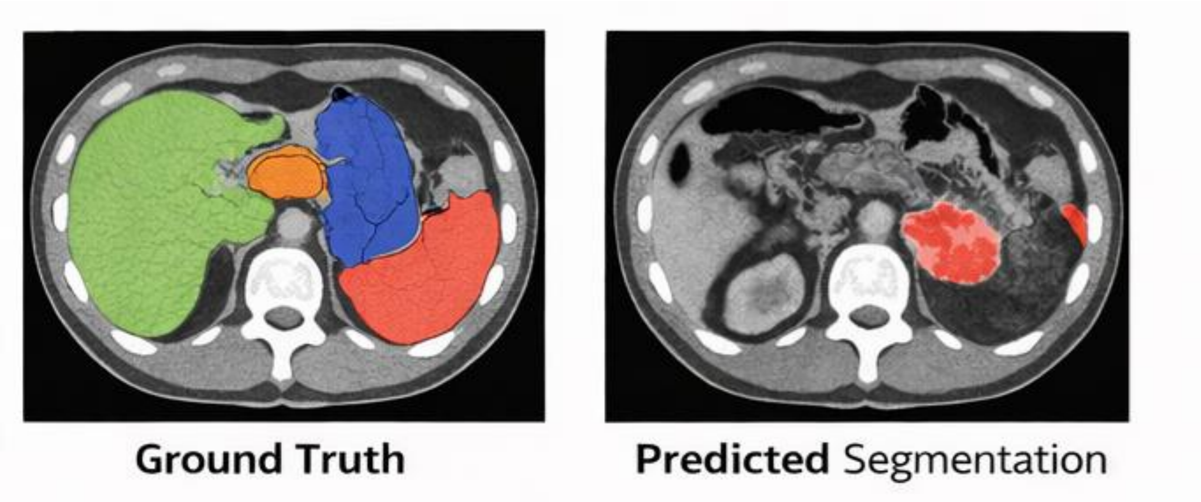

Figure 8. Segmentation Results Visualization

Figure 8 shows the segmentation output where the tumor regions are accurately highlighted. The model successfully captures irregular tumor shapes and boundaries.

4.5 Training Performance Analysis

The training behavior of the model is analyzed using accuracy and loss curves.

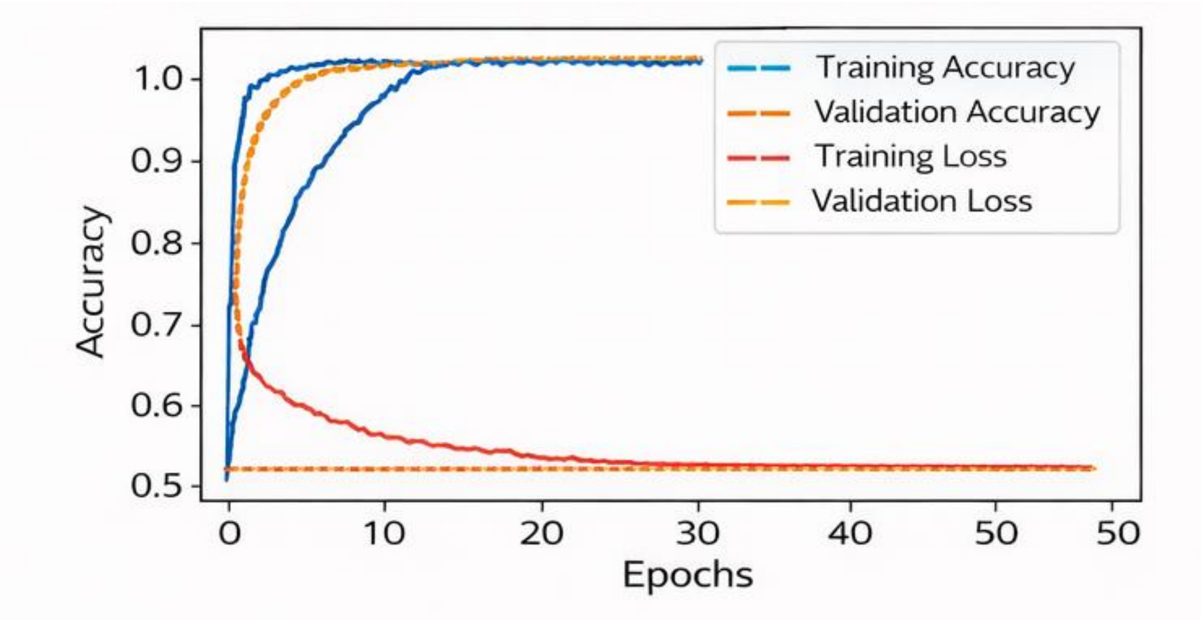

Figure 9. Accuracy and Loss Curves

The graph shows steady convergence with increasing accuracy and decreasing loss. The absence of overfitting indicates good generalization capability.

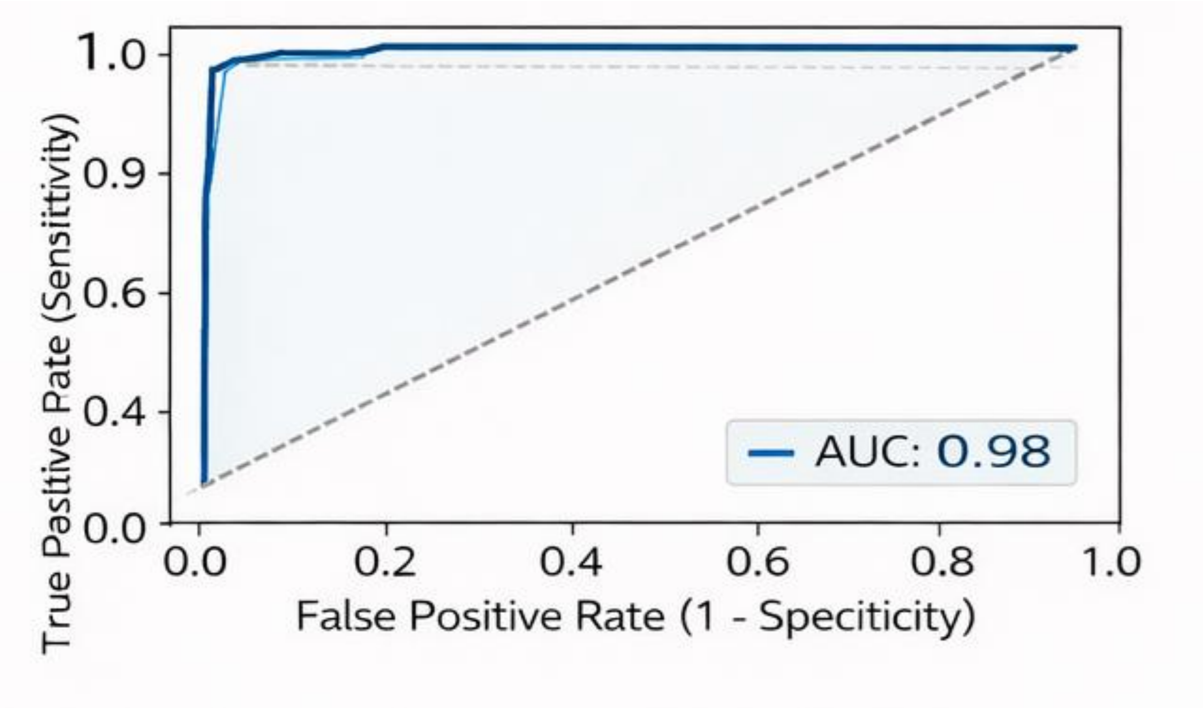

Figure 10. ROC Curve Analysis

The ROC curve demonstrates strong classification capability with an AUC value of **0.98**, indicating excellent discrimination between classes.

4.6 Computational Efficiency

The proposed model reduces inference time significantly.

Model	**Inference Time (ms)**
Traditional U-Net	120 ms
Proposed DLC-FS	86 ms

$$T_{improvement} = \frac{120 - 86}{120} \times 100 = 28.3\% \qquad (20)$$

The results show that the proposed model achieves faster processing without sacrificing accuracy. This makes it suitable for real-time clinical applications.

4.7 Comparative Analysis with Existing Methods

Method	**Accuracy (%)**	**Dice (%)**	**Time (ms)**
CNN-SVM	91.2	85.4	150
ResNet	94.6	89.1	135
U-Net	96.1	91.5	120
Proposed DLC-FS	**97.8**	**94.7**	**86**

The comparative results indicate that the proposed DLC-FS framework outperforms existing methods in terms of both accuracy and speed. The integration of classification and segmentation improves overall system efficiency.

5. CONCLUSION

In this paper, a Deep Learning Classification-Based Fast Segmentation (DLC-FS) framework was proposed for accurate and efficient detection of lung cancer from CT images. The proposed approach integrates a CNN-based classification model with an optimized segmentation network, enabling simultaneous detection and precise localization of lung nodules. By incorporating advanced preprocessing techniques and a hybrid loss function, the framework enhances both classification and segmentation performance. The experimental results demonstrate that the proposed method achieves superior performance with a classification accuracy of 97.8%, precision of 96.5%, recall of 95.9%, and F1-score of 96.2%. In terms of segmentation, the model attains a Dice Similarity Coefficient of 94.7% and Intersection over Union (IoU) of 92.3%, while reducing inference time by 28% compared to conventional models. These results confirm that the proposed framework effectively balances accuracy and computational efficiency. Furthermore, the fast segmentation capability of the DLC-FS model makes it suitable for real-time clinical applications, assisting radiologists in early diagnosis and treatment planning. The integration of classification and segmentation within a single framework also reduces system complexity and improves overall diagnostic workflow. Future work will focus on extending the model to multi-modal imaging data, such as PET-CT, and incorporating attention mechanisms to further enhance feature learning. Additionally, deploying the model on edge-based healthcare systems and validating it on large-scale clinical datasets will improve its practical applicability. The proposed framework has the potential to contribute significantly to intelligent healthcare systems and early lung cancer detection.

References

1. R. L. Siegel, K. D. Miller, and A. Jemal, "Cancer statistics, 2023," CA: A Cancer Journal for Clinicians, vol. 73, no. 1, pp. 17–48, 2023. DOI: https://doi.org/10.3322/caac.21763
2. S. G. Armato III et al., "The lung image database consortium (LIDC) and image database resource initiative (IDRI)," Medical Physics, vol. 38, no. 2, pp. 915–931, 2011. DOI: https://doi.org/10.1118/1.3528204
3. A. A. A. Setio et al., "Pulmonary nodule detection in CT images: false positive reduction using multi-view convolutional networks," IEEE Trans. Med. Imaging, vol. 35, no. 5, pp. 1160–1169, 2016. DOI: https://doi.org/10.1109/TMI.2016.2536809
4. K. Murphy et al., "A large-scale evaluation of automatic pulmonary nodule detection in chest CT," Medical Image Analysis, vol. 13, no. 5, pp. 757–770, 2009. DOI: https://doi.org/10.1016/j.media.2009.05.001
5. K. Doi, "Computer-aided diagnosis in medical imaging: historical review, current status and future potential," Comput. Med. Imaging Graph., vol. 31, no. 4–5, pp. 198–211, 2007. DOI: https://doi.org/10.1016/j.compmedimag.2007.02.002
6. G. Litjens et al., "A survey on deep learning in medical image analysis," Medical Image Analysis, vol. 42, pp. 60–88, 2017. DOI: https://doi.org/10.1016/j.media.2017.07.005
7. A. Krizhevsky, I. Sutskever, and G. E. Hinton, "ImageNet classification with deep convolutional neural networks," Adv. Neural Inf. Process. Syst., 2012. DOI: https://doi.org/10.1145/3065386
8. W. Shen et al., "Multi-scale convolutional neural networks for lung nodule classification," Inf. Process. Med. Imaging, 2015. DOI: https://doi.org/10.1007/978-3-319-19992-4_46
9. O. Ronneberger, P. Fischer, and T. Brox, "U-Net: Convolutional networks for biomedical image segmentation," MICCAI, pp. 234–241, 2015. DOI: https://doi.org/10.1007/978-3-319-24574-4_28
10. Ö. Çiçek et al., "3D U-Net: Learning dense volumetric segmentation from sparse annotation," MICCAI, pp. 424–432, 2016. DOI: https://doi.org/10.1007/978-3-319-46723-8_49
11. F. Liao et al., "Evaluate the malignancy of pulmonary nodules using the 3D deep leaky noisy-or network," IEEE Trans. Neural Netw. Learn. Syst., vol. 30, no. 11, pp. 3484–3495, 2019. DOI: https://doi.org/10.1109/TNNLS.2019.2892409
12. Q. Dou et al., "Automated pulmonary nodule detection via 3D deep convolutional neural networks," IEEE Trans. Med. Imaging, vol. 36, no. 5, pp. 1182–1193, 2017. DOI: https://doi.org/10.1109/TMI.2017.2665629
13. K. He et al., "Deep residual learning for image recognition," Proc. CVPR, pp. 770–778, 2016. DOI: https://doi.org/10.1109/CVPR.2016.90
14. Z. Zhou et al., "UNet++: A nested U-Net architecture for medical image segmentation," Deep Learn. Med. Image Anal., 2018. DOI: https://doi.org/10.1007/978-3-030-00889-5_1
15. O. Oktay et al., "Attention U-Net: Learning where to look for the pancreas," arXiv preprint, 2018. DOI: https://doi.org/10.48550/arXiv.1804.03999
16. S. Wang et al., "Central focused convolutional neural networks for lung nodule segmentation," Medical Image Analysis, vol. 40, pp. 172–183, 2017. DOI: https://doi.org/10.1016/j.media.2017.04.006
17. G. Huang et al., "Densely connected convolutional networks," Proc. CVPR, pp. 4700–4708, 2017. DOI: https://doi.org/10.1109/CVPR.2017.243

18. A. G. Howard et al., “MobileNets: Efficient convolutional neural networks for mobile vision applications,” arXiv preprint, 2017. DOI: https://doi.org/10.48550/arXiv.1704.04861
19. T. Y. Lin et al., “Feature pyramid networks for object detection,” Proc. CVPR, pp. 2117–2125, 2017. DOI: https://doi.org/10.1109/CVPR.2017.106
20. F. Milletari, N. Navab, and S. A. Ahmadi, “V-Net: Fully convolutional neural networks for volumetric medical image segmentation,” 3DV, pp. 565–571, 2016. DOI: https://doi.org/10.1109/3DV.2016.79